Mon. Not. R. Astron. Soc. **326,** 950–958 (2001)

Starspot patterns on the M dwarfs HK Aqr and RE 1816 +541

J. R. Barnes[1,2]★ and A. Collier Cameron[2]
[1]*Centro de Astrofísica da Universidade do Porto, Rua das Estrelas, 4150 Porto, Portugal*
[2]*School of Physics and Astronomy, University of St Andrews, St Andrews KY16 9SS*

Accepted 2001 May 2. Received 2001 April 23; in original form 2000 December 29

ABSTRACT

We present the first Doppler images of two M dwarfs in the solar neighbourhood. Late-type dwarfs are generally too faint to enable spectra with sufficient signal-to-noise (S/N) ratios for Doppler imaging to be obtained in short enough exposure times. Using the large number of photospheric absorption lines in each spectrum, we apply *least-squares deconvolution* to derive composite line profiles with S/N ratios of 100–500. The surface images of HK Aqr reveal a moderately spotted surface, with the majority of starspots appearing at low latitudes, whereas RE 1816 +541 exhibits spots at all latitudes. Neither star shows significant evidence for the oft-observed polar spot. Despite the boost in S/N ratio achieved with the least-squares deconvolution technique, the images are not consistent enough to determine reliably the magnitude of differential rotation. Nevertheless, the images are consistent enough to place upper limits on the rate of surface shear.

Key words: line: profiles – methods: data analysis – stars: activity – stars: imaging – stars: late-type – stars: spots.

1 INTRODUCTION

Deriving surface images by fitting distortions in Doppler-broadened photospheric absorption profiles has proved to be a very valuable tool since it was first successfully applied by Vogt & Penrod (1983) to the RS CVn system HD 1099. A number of rapidly rotating stars including giants, RS CVn binaries, main-sequence and T Tauri stars have been mapped in temperature distribution, whereas Ap stars have been mapped in chemical abundance. Yet, there still remain areas of parameter space available to Doppler imaging, which have not been studied owing to the constraints of the technique. The maximum-entropy regularization requires a S/N ratio of at least 200–300 to reliably constrain an image solution with the typical spot sizes found in main-sequence dwarfs. Combined with the desire to keep observational exposure times to a minimum, observations of objects with typically 0.5-d axial rotation periods have been restricted to those objects with $m_v \leq 8$.

Least-squares deconvolution, a technique first implemented for use on polarimetric Stokes *V* spectra (Donati et al. 1997) makes use of a large number of lines in a typical échelle spectrum. This technique allows a single high S/N ratio profile, with multiplex gain factors of typically >20 on the original spectrum, to be derived from thousands of spectral lines at each observation phase. Donati & Collier Cameron (1997) showed how the resulting low-noise profiles could be used to derive maps with greater detail than previously attained. By tracking starspots from images separated by several nights, measures of the sense and magnitude of the differential rotation rate were made. The technique has subsequently been applied to a number of objects such as G dwarfs ($m_v \simeq 11.5$) in the α Persei cluster (Barnes et al. 1998), and to main-sequence solar neighbourhood dwarfs (Barnes et al. 2000; Barnes, Collier Cameron & James 2001). Typical S/N ratios of the order of 1000 have been achieved. Essentially, the technique opens up the possibility of studying intrinsically faint objects with telescopes of intermediate (2–4 m) aperture. The purpose of this paper is to present an analysis of the feasibility of applying least-squares deconvolution to M dwarfs, and to present images for two previously well-studied objects. Four-metre class telescopes with current échelle spectrographs restrict viable targets to those with $m_v \leq 13$. This essentially excludes the possibilities of studying M dwarf spectra in young open clusters such as α Persei which have $m_v \simeq 14$–15. There are only two well-studied M dwarfs in the solar neighbourhood, the southern object HK Aqr (Gl 890) and the northern object RE 1816 +541.

HK Aqr is a rapidly rotating star with an equatorial rotation velocity of $\sim$70 km s^{-1} (Young, Skumanich & Harlan 1984). Axial rotation periods from photometric modulations of 0.4312 d (Pettersen et al. 1987) and 0.4307 d (Young et al. 1990) have been determined. An analysis of previous photometric measurements by Bopp et al. (1988) revealed an average $m_v = 10.85$ with variations always within 0.05 mag. The photometric amplitude at a given epoch, however, can vary by as much as 0.15. The waxing and waning of long-lived polar spots was suggested as an explanation for the observed small changes in brightness and colour. Young et al. (1990) also proposed high-latitude activity in

★E-mail: jrb3@st-andrews.ac.uk

order to explain the lightcurve morphology. The spectral type of dM1.5e has been determined by Pettersen et al. (1987), while an *Hipparcos* parallax of 45.75 ± 2.60 milliarcsec yields a distance of 21.86 ± 1.24 pc.

Flaring activity has been reported by Pettersen et al. (1987), and in Hα by Herbst & Layden (1987) and Byrne, Eibe & Rolleston (1996). The latter of these studies revealed a series of Hα absorption transients, attributed to a system of prominences located below the corotation radius. Further indications of chromospheric and coronal activity come from *EXOSAT* observations, which indicate a steady X-ray emission (Rao & Singh 1990).

The ROSAT EUV Wide Field Camera source, RE 1816 +541 was detected at the position RA 18 h 16 m 19.1 s, December +54 10 26 (J2000.0) with a positional error of 63 arcsec and count rates of 6×10^{-3} s^{-1} (Pounds et al. 1993). This has been identified with the object GSC 3904.00967, or EY Dra. The first detailed analysis of optical data was carried out by Jeffries, James & Bromage (1994) who identified RE 1816 +541 as a dM1 or dM2 object based upon the strength of its molecular MgH and TiO bands. Optical spectra were secured on three occasions using the Intermediate Dispersion Spectrograph at the Isaac Newton Telescope. These observations confirmed chromospheric activity in the form of Ca II H and K emission lines and Hα emission, a radial velocity, $v_r = -21.9 \pm 1.5$ km s^{-1} and projected equatorial rotation velocity, $v \sin i = 61 \pm 1.5$ km s^{-1}. An axial rotation period of 0.4589 d has been determined (Robb & Cardinal 1995) from *V*-band photometric data. More recently, the Hα line of RE 1816 +541 has been studied in detail (Eibe 1998) which indicates, as in the case of HK Aqr, the presence of prominence clouds below the corotation radius. A very strong flare was also detected from pronounced enhancement of emission lines, and dilution of photospheric absorption lines.

2 OBSERVATIONS AND DATA REDUCTION

The present observations are taken from the ING and AAO data archives. The spectrograph setups in both cases were optimized for study of the strong Hα line that appears in emission on both stars. HK Aqr was observed at the 3.9-m Anglo Australian Telescope (AAT) with the University College London Échelle Spectrograph (UCLES) on 1991 August 24–26, using the 1k × 1k Thomson charge-coupled device (CCD). The seeing conditions varied over the three nights of observing and were generally of insufficient quality to justify extraction on August 25. The wavelength range of extracted spectra is 4855–6730 Å. Full details of instrumental setup, seeing conditions and observations are given in Byrne et al. (1996). Observations of RE 1816 +541 were made at the 4.2-m William Herschel Telescope (WHT) at the Isaac Newton Group of Telescopes on La Palma, using the Utrecht Échelle Spectrograph (UES) and the 1k × 1k TEK 3 CCD. A redder setting with a wavelength coverage of 5351–9085 Å was used in this instance (see Eibe 1998 for further details). The exposure lengths were 300 s for all observations of both objects. For the purposes of least-squares deconvolution, we generally take an atmospheric cut-off of 7000–7500 Å where telluric lines become numerous. The vast majority of useful lines are to be found at bluer wavelengths.

Individual spectra were bias corrected prior to extraction using standard Starlink FIGARO routines. The Starlink package ECHOMOP, developed by Mills (1994), was used to flat-field and extract the échelle orders from each CCD frame. The scattered light was modelled and the orders optimally extracted using the routine developed by Horne (1986). The thorium-argon arc-frames used for wavelength calibration were also extracted in conjunction with a target spectrum, and calibrated using ECHOMOP.

3 LEAST-SQUARES DECONVOLUTION OF M DWARF SPECTRA

The process of determining continuum fits to spectra has been described extensively in previous papers (Barnes et al. 2000). All spectra were deconvolved at the CCD pixel resolution using our routine SPDECON. For the HK Aqr data (Thomson CCD), the deconvolved velocity bin size is 2.5 km s^{-1}, whereas for the RE 1816 +541 data, the corresponding bin size is 3 km s^{-1}. The technique of least-squares deconvolution requires a line list, generated from model atmospheres, which contains the wavelength positions and line depths of rotationally unbroadened absorption profiles. A solution is obtained by finding the best fit of the convolution of the profile to be determined with the line-list to the observed spectrum (Donati et al. 1997). M dwarf spectra contain molecular absorption bands, the opacities for which are poorly represented in most available model atmospheres. This immediately raises the question as to the suitability of the available line-lists as it is not clear whether the least-squares profile will be distorted because of underestimation in the number of lines. To this end, we have performed tests using synthetic data.

An artificial échelle spectrum was generated using a $T = 4000$ K line list (Vienna Atomic Line Database; Kupka et al. 1999), an empirical rotation profile (Gray 1992) and the wavelength calibration file obtained for the RE 1816 +541 data set. Least-squares deconvolution was then applied using line lists with

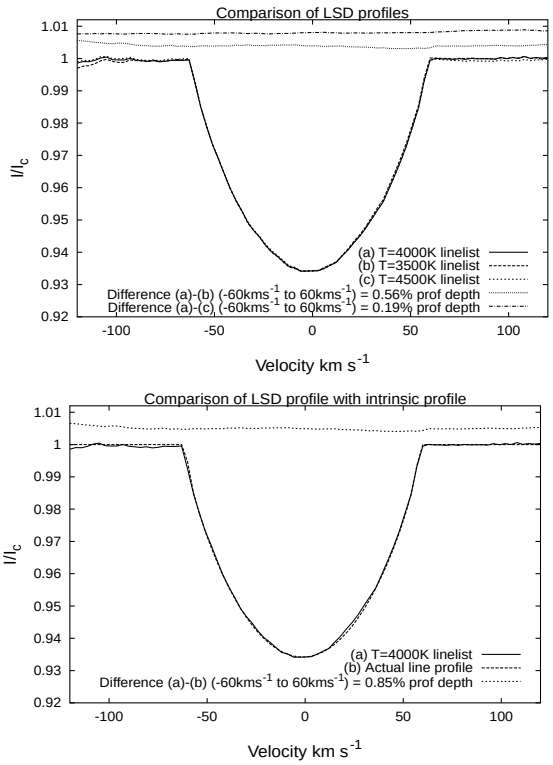

Figure 1. Testing the robustness of least-squares deconvolution. As can be seen, the deconvolved profile shape is relatively independent of the line list used for $\Delta = \pm 500$ K). The mismatch of the deconvolved profile derived using the correct line list when compared with the intrinsic profile introduces a greater deviation, but of the same order of magnitude

$T = 3500$, 4000 and 4500 K. The results are shown in Fig. 1 and reveal that use of an incorrect line list does not severely affect the shape of the deconvolved profile. Compared with the $T = 4000$ K deconvolved profile, average deviations of less than 1 per cent of the profile depth, across the profile are found, being of similar magnitude to the uncertainties of the deconvolution process itself. This test is not ideal since it merely demonstrates the consequences of using incorrect representations of *atomic* line data, and not omission of *molecular bands*. Given the robustness of the technique to these effects, however, we are confident that any unrepresented molecular lines do not distort the deconvolved profile. Lines in the regions of known strong TiO bands (such as at 6782, 7055 and 7126 Å) are removed from the line list, as naturally are the regions around the strongest atomic lines such as hydrogen Balmer (6555–6570 Å) and Na D (5875–5905 Å).

Least-squares deconvolution was applied to all spectra in both data sets. Fig. 2 shows the input and output S/N ratio statistics for the process. In the case of HK Aqr, a total of 938 absorption lines (no repeated lines in adjacent orders) were available. The input spectra vary in quality with some very poor S/N ratio data at the times when the star was at low altitude and the seeing poor. The mean profiles have S/N ratios varying from 100–450, yielding an average increase in S/N ratio by a factor of 31.6. Even after deconvolution, the data from August 24, are still very poor for Doppler imaging purposes. The RE 1816 +541 data set is of higher quality, but with fewer available absorption lines (529 with 11 lines repeated in adjacent orders). The majority of output profiles have S/N ratio values in the range 300–500. The two straight lines represent the mean gain (lower dot-dash line) and the maximum achievable gain, the latter being approximately (number of lines)$^{1/2}$. A comparison reveals a 20 per cent greater gain efficiency in the lower input S/N ratio HK Aqr data set, indicating a non-linearity of gain efficiency with input S/N ratio, in agreement with the findings of Donati et al. (1997).

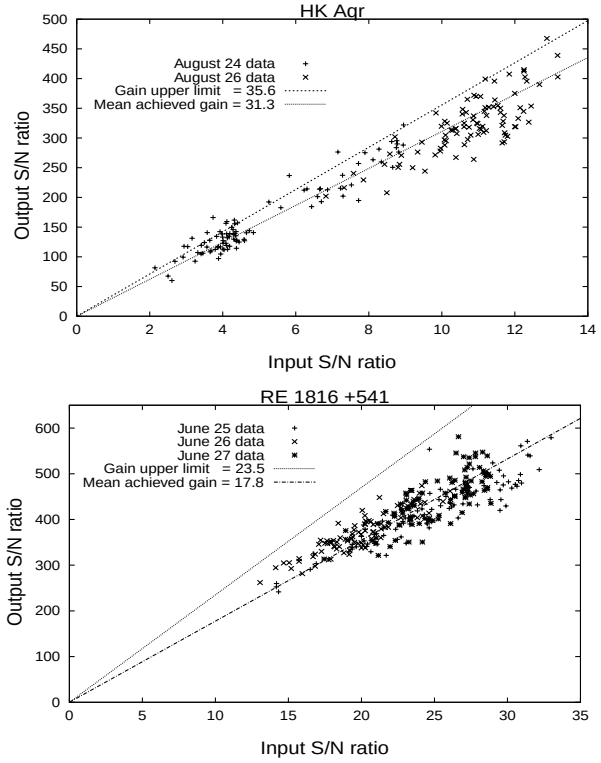

Figure 2. Plots showing the mean input S/N ratio of the deconvolved spectra (over the portion of spectrum used in deconvolution) against the output S/N ratio of each profile. The upper line in each plot represents the maximum attainable S/N ratio (i.e. (number of lines used)$^{1/2}$). The lower straight line represents the mean gain attained as calculated from all points. The process is therefore more efficient for lower input S/N ratio spectra.

4 RESULTS

4.1 Stellar parameters

The parameters that best fit the data are given in Table 1 for both objects, and are in good agreement with previous estimates. The most difficult parameter to determine is the axial inclination, especially for M dwarfs, which may not have accurate parallax measurements or which may show fluctuating absolute magnitudes and colours. The method of minimizing the χ^2 parameter for axial inclination only works well with high S/N ratio data. In the case of low S/N ratio, tests on synthetic data reveal that the inclination is always biased to low values.

The temperature and luminosity of HK Aqr, as determined from the brightest measurements lead to values of axial inclination in excess of 90°. Using the colour-temperature transformation of Soderblom et al. (1993) with $B–V = 1.43$ results in a temperature of $T = 3870$ K; which with an absolute magnitude of $m_v = 10.83$, and parallax of 45.75 ± 2.60 milliarcsec, yields a luminosity of $\log(L/\mathrm{L}_\odot) = -1.3654 \pm 0.05$. The resulting radius, $R = 0.4678\,\mathrm{R}_\odot$ is clearly incompatible with the $R \sin i = 0.5872\,\mathrm{R}_\odot$ value determined from $v \sin i$ and P, since this leads to $\sin i = 1.26 \pm 0.08$. A means of correcting this problem arises if we assume that the star is heavily spotted. For a global, unresolved 40 per cent spot filling factor, the absolute magnitude of $M_v = 9.11$ is overestimated by 0.49, assuming spots of mean temperature 1500 K cooler than the photospheric temperature. A recalculation of the radius then gives $\log(L/\mathrm{L}_\odot) = -1.16$ and $R = 0.5859\,\mathrm{R}_\odot$ leading to $\sin i = 1.00 \pm 0.062$. This high degree of spottedness has been discussed in previous papers (Barnes et al. 2000) and is consistent with the high degree of starspot coverage determined from TiO bands on earlier type dwarfs (O'Neal, Neff & Saar 1998). Whatever the *true* axial inclination, it is certainly high, with this correction giving an estimate in the range $90° > i > 70°$. For the purposes of reconstruction, discrepancies of 10° have very little effect in the resulting images. Features are reflected in both hemispheres at high latitudes greater than 70°. In order to keep this degeneracy in the solution to a minimum, we have reconstructed images at an inclination of 75° for HK Aqr.

There is no parallax measurement to aid an axial inclination determination for RE 1816 +541. As discussed by (Jeffries et al. 1994), based upon the radial velocity alone (-21.72 ± 0.05) it seems likely that RE 1816 +541 is a member of the Local Association, which predicts a value of $-25.0\,\mathrm{km\,s^{-1}}$. Given the assumption that the age of RE 1816 +541 is 50 Myr, a value of

Table 1. System parameters for HK Aqr and RE1816 +541. $\Delta\chi^2 = 1$ errors are given

	HK Aqr	RE 1816 +541
v_r	$6.60 \pm 0.04\,\mathrm{km\,s^{-1}}$	$-21.72 \pm 0.05\,\mathrm{km\,s^{-1}}$
P	0.4307 ± 0.0005 d	0.4586 ± 0.0002 d
$v \sin i$	$69.0 \pm 0.1\,\mathrm{km\,s^{-1}}$	$61.6 \pm 0.2\,\mathrm{km\,s^{-1}}$
i	70–90°	66–90°

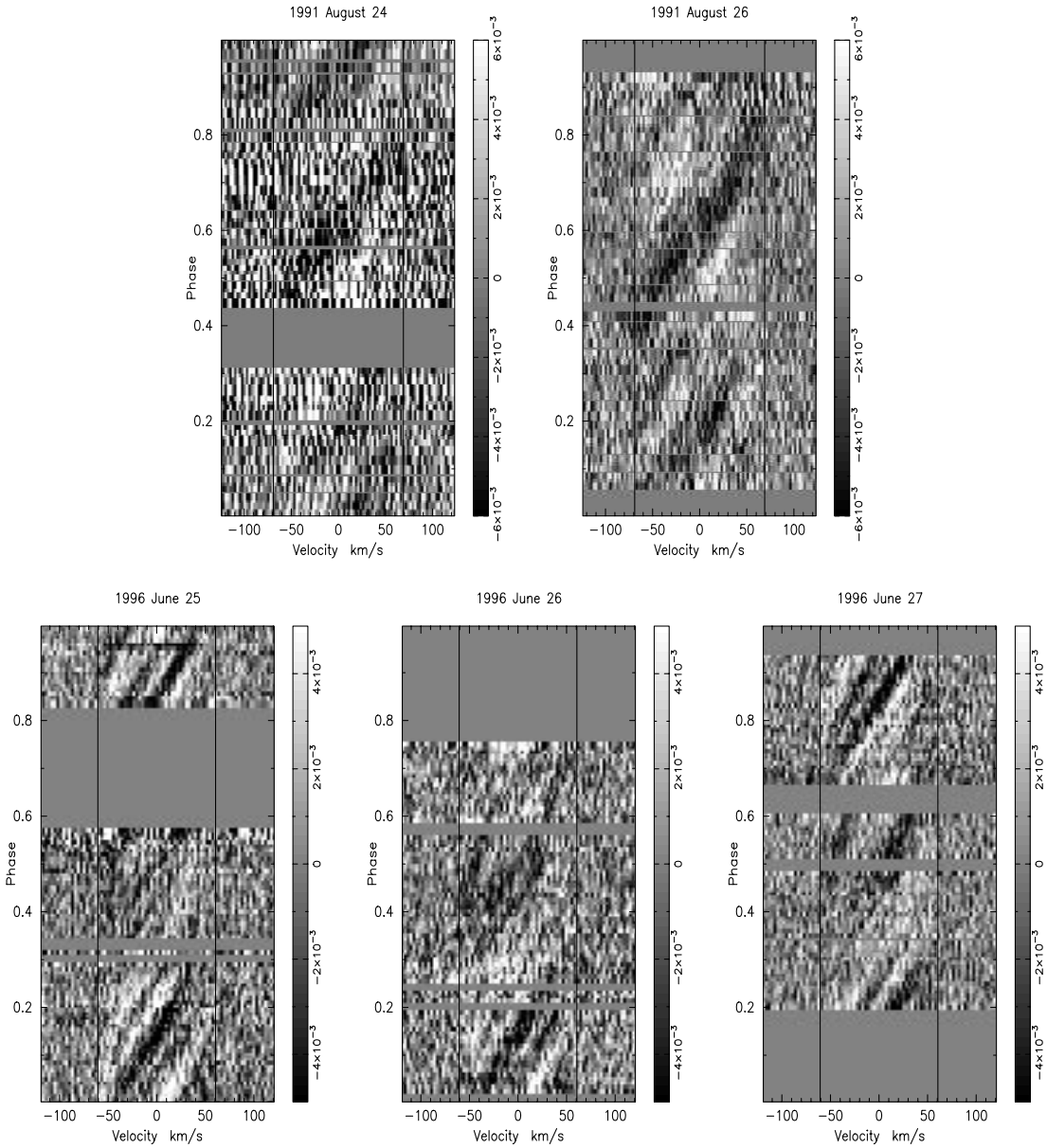

Figure 3. HK Aqr (top) and RE 1816 +541 (bottom) grey-scale time-series images of the deconvolved spectra for each night of observations. Phase is plotted against deconvolved velocity (zero-corrected) bin. The spectra are mean profile subtracted hence the white features which represent starspot signatures. The $v \sin i$ limits are marked by black vertical lines.

$\log(L/\mathrm{L}_\odot) = -1.114 \pm 0.039$ is obtained from (D'Antona & Mazzitelli 1994), which yields $M_v = 8.54 \pm 0.12$. Hence an estimate of $D = 45.5 \pm 2.1$ pc is obtained. A value of $R = 0.601 \pm 0.034\,\mathrm{R}_\odot$ is determined and the theoretical temperature $T = 3900 \pm 100$ K, is in good agreement with that determined from the $B - V$ colour ($T = 3850$ K). Given the empirically determined $R \sin i = 0.549 \pm 0.002\,\mathrm{R}_\odot$, an axial inclination of $i = 66°$ is determined (with $75° > i > 60°$). For the purposes of image reconstruction, an axial inclination of $i = 70°$ was used.

4.2 HK Aqr

The time-series spectra after least-squares deconvolution are shown in Fig. 3. Despite the poor quality of the August 24 data, starspot signatures are clearly visible and seen repeated on August 26. A further complication of solar spectrum contamination results from intermittent cloud and a nearby moon during the observations. Donati et al. (2000) removed similar contamination from spectra by assuming that a linear combination of the solar spectrum and *uncontaminated* object spectrum could be used to fit each spectrum. A least-squares fit allows the contribution from each component to be calculated and hence, the solar component can be removed. However, we found that all spectra were contaminated by the solar spectrum and did not have the luxury of a solar spectrum obtained from the moon. A similar although slightly convoluted procedure was attempted on the deconvolved spectra. Parameter minimization was performed on the deconvolved data with the central badly affected pixels excluded from the fits. The determined parameters v_{rad}, and $v \sin i$ should largely be unaffected by this procedure since the values will be largely determined by the overall profile shape. A mean profile was generated with these parameters. This was used in combination

with the deconvolved profile of a slowly rotating G1V standard star to represent and remove the solar contribution using the same procedure as outlined above. The technique appears to work well, but the cleaned spectra cannot be totally independent of the chosen parameters used to represent the mean stellar profile. A polar spot would truncate the centre of the profile, so the immaculate mean profile used could result in underestimation of the solar profile contribution. Overestimation of the solar profile contribution is unlikely, and only for a 50 per cent overestimation is a polar spot of any significance reconstructed.

The maximum-entropy regularized images are shown in Fig. 4 and reflect the quality of data on both nights. Although there is considerable phase overlap, individual features are not repeated in detail. It will be noted from Fig. 2 that the S/N ratio in the majority of profiles from August 24 clusters around values of 125, which calls into question the ability of the maximum-entropy regularization to reliably constrain an image. Certainly, the global spot structure is consistent with the August 26 image, with many features being identifiable in both images, albeit with different morphologies. The fact that the August 26 data constrain the more reliable image is born out in the combined image, which closely resembles this image. The lack of high-latitude features is quite striking when one compares the images with other images of young rapid rotators found in the literature. This lack of high-latitude structure is at least in part caused by the low S/N ratio of the data. Given the axial inclination of HK Aqr, high latitudes appear severely foreshortened and cross smaller, central regions of the rotation profile only, as the star rotates. Any starspot signatures

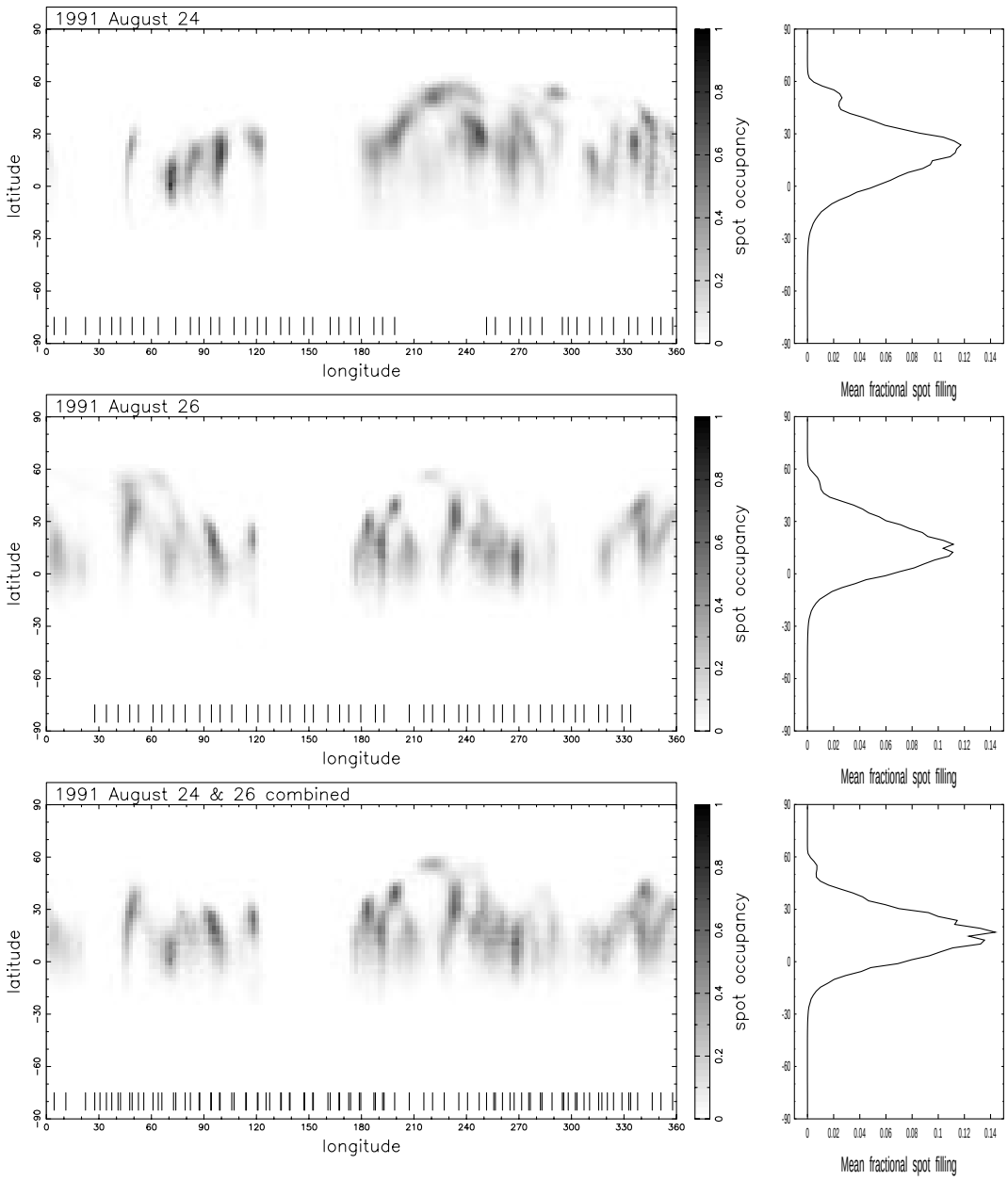

Figure 4. From top to bottom: HK Aqr Mercator maps for the nights of 1991 August 24, 26 and 24 and 26 combined. The resolution of the images is 2.25 deg pixel^{-1}. The tick marks indicate the phases of observation. The plot to the right of each map is a representation of the mean spot filling as a function of latitude.

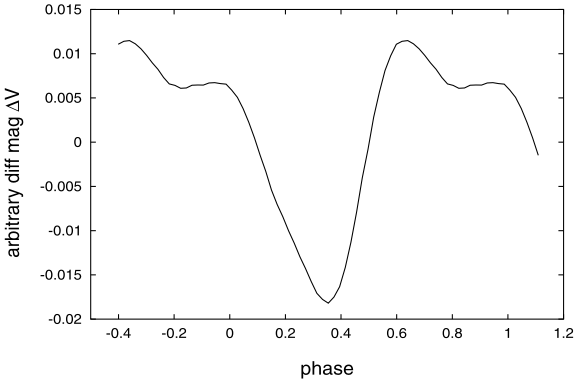

Figure 5. HK Aqr simulated lightcurve from spectroscopic data using 1991 August 25 and 26 image.

possess smaller amplitudes, are poorly resolved, and in this case, lost completely in the noise. This subject is explored further in Section 5 with tests using fake images to generate low S/N ratio profiles.

These findings are in contrast with the conclusions presented by Young et al. (1984) who concluded that the spot features on HK Aqr were located at high latitudes. This conclusion was reached from analysis of *V*-band photometric data and study of the Hα line. The lightcurve was interpreted by these authors as being the result of two active regions separated by 180°. The Hα variations were interpreted as being the result of high-latitude plage regions, which were sheared owing to significant amounts of differential rotation. Although this interpretation added further weight to the high-latitude spot coverage, the explanation of the Hα variations being the result of circumstellar prominences (Collier Cameron & Robinson 1989a,b) have gained acceptance. As stated above, the present archival data set was initially obtained for the study of the Hα line, the authors (Byrne et al. 1996) finding a system of prominences within the corotation radius.

The current spectroscopic data yield images of HK Aqr that clearly contradict the idea of significant high-latitude features. Using the combined image reconstruction of HK Aqr (Fig. 4), a photometric *V*-band lightcurve has been generated. Generally, one would prefer to include photometric data into an initial image reconstruction in order to further constrain an image. Photometric data are most beneficial in constraining low-latitude features where the stellar surface pixels suffer from little foreshortening. There is often a discrepancy between the amplitude of the photometric lightcurve and the surface spot filling factors derived from the spectroscopic data. A number of factors may be at play here, such as smearing of low-latitude features (owing to greater uncertainties in the associated features which move quickly through the stellar line profile), unresolved spot coverage and a tendency for the maximum-entropy regularization result in a slight underestimation of spot filling.

The resulting lightcurve (note that phase runs in the opposite sense to longitude) is shown in Fig. 5 and reveals a minimum in brightness associated with the most heavily spotted region (phase $\sim$0.35, longitude $\sim$235°). A second dip in the lightcurve is revealed at phase $\sim$0.83 (longitude 60°). The amplitude of $\sim$0.03 is, however, of the same magnitude as seen in fig. 3 in Young et al. (1984). One factor which led to the interpretation of these authors was the apparent asymmetry, with the increase to maximum light being much steeper than the decrease to minimum light. This asymmetry can clearly be reproduced by all features occurring at low to intermediate latitudes, but with differing spot filling factors as a function of longitude.

The change in amplitude of the lightcurve can be attributed to two possibilities. First, two main spot groups with relatively clean photosphere between will reduce the variation in luminosity if parts of both groups are visible at certain times. Hence, a double-peaked lightcurve will be seen. A single spot group will result in a single-peaked lightcurve of greater amplitude. The second reason may be the result of the region of active latitudes changing during a possible stellar magnetic cycle. A single-peaked curve of low amplitude would add support to this second hypothesis. In reality, surface temperature inhomogeneities cannot be constrained by photometric data alone. Only long-term studies of HK Aqr, simultaneously at different wavelengths will allow some of these points to be affirmed or rejected.

4.3 RE 1816 +541

The RE 1816 +541 deconvolved profiles being of higher quality make identification of starspot features easier. The time-series spectra in Fig. 3, show several features repeated from one night to the next. The resulting images are shown in Fig. 6 and once again show similarities and differences from one night to the next. The starspot complex centred around longitude 230°, latitude 40° reveals a slightly different morphology from night to night despite always being well sampled in observations. The idea of starspot evolution is questionable given the moderate S/N ratio of the spectra and moderate $v \sin i$ (and hence the number of resolution elements) of the profiles. It is clear, however, that despite some high-latitude structure, like HK Aqr, RE 1816 +541 exhibits no strong polar spot at the time of observations. Starspots are located at all latitudes, with the majority of features being evenly distributed in the range 20°–80°.

5 DIFFERENTIAL ROTATION

Efforts to measure the latitudinal differential rotation from pairs of Doppler images have met with varying degrees of success. The most convincing results that measure both the magnitude and sense of the differential rotation (assuming a solar-type law) have come from data sets that provide high S/N ratios, high-$v \sin i$ profiles and good phase coverage (e.g. Donati & Collier Cameron 1997; Donati et al. 2000). Further attempts have yielded results with some success (Barnes et al. 2000), or have only resulted in estimates of upper limits on the differential rotation (Barnes et al. 2001).

In an attempt to ascertain the reliability of the derived images, synthetic data sets with the same parameters and the same S/N ratio were created from an 'ideal', synthetic image of RE 1816 +541. Images reconstructed from the data sets (which differ only in the random noise pattern) reveal that at a S/N ratio of 350, the features are not always consistently reproduced. Features above 40° latitude especially are less consistent, indicating that any potentially measurable profile distortions are strongly affected by noise. A S/N ratio of 1000, however, yields much more reliable images, up to latitudes of 70°. These results demonstrate the arguments put forward in Section 4.1. By generating 100 data sets for S/N ratios of 350 (data set 1) and 1000 (data set 2) and cross-correlating all possible combinations at each S/N ratio value, a measure of the degree of uncertainty in longitudinal position can be obtained (Fig. 7). By considering the resulting mean cross-correlation peak width for each data set and accounting for the width of the intrinsic

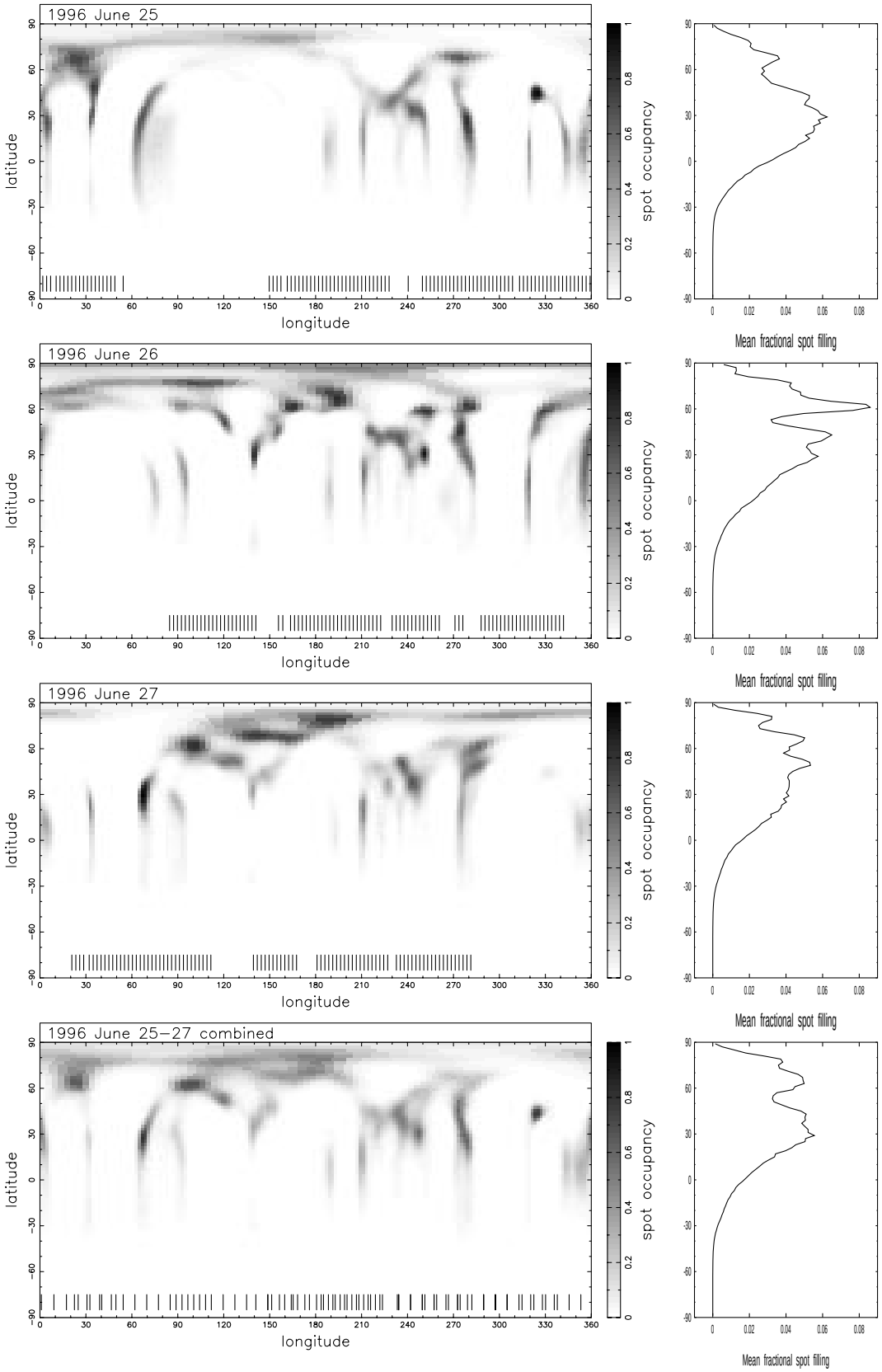

Figure 6. Top to bottom: RE1816 +541 Mercator maps for the nights of 1996 June 25–27 and all nights combined. The tick marks indicate the phases of observation. The plot to the right of each map is a representation of the mean spot filling as a function of latitude.

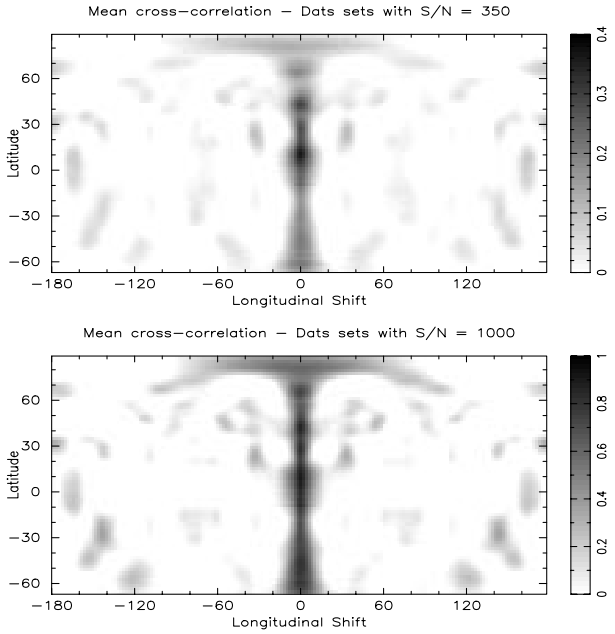

Figure 7. Cross-correlation images for S/N ratio = 350 data sets (top) and S/N ratio = 1000 data sets (bottom).

mean auto-correlation peaks, longitudinal uncertainties of ±6.3° and ±4.5° are obtained for data sets 1 and 2, respectively. These values are not greatly different since for lower S/N ratio values, the starspot is smeared to a greater extent in latitude, which results in a contraction in longitudinal extent (as the starspot area is approximately conserved). A comparison of these results with the commonly measured rates of differential rotation can be made. Measurements which yield equator-lap-pole times of 50–110 d have been made on the T Tauri star RX J1508.6-4423 (Donati et al. 2000) and AB Dor (Donati & Collier Cameron 1997). The above uncertainties translate into limits for equator-lap-pole times of 28.7 and 39.7 d per day separating the observations, for data sets 1 and 2, respectively. For RE 1816 +541, the maximum separation of images is 2 d, which gives an upper limit of 58 d for the current data set.

We have Incorporated a solar-type differential rotation law into our Doppler imaging program, allowing for adjustment of shift (Ω_0) and shear ($\Delta\Omega$) parameters in the relation

$$\Omega(\theta) = \Omega_0 - \Delta\Omega \sin^2(\theta), \tag{1}$$

where θ is the stellar latitude. The plots of $\Delta\chi^2$ as a function of Ω_0 versus $\Delta\Omega$ in Fig. 8 show a correlation between the two parameters. As expected from the above analysis, the χ^2 surface is irregular on a small scale, making accurate measurements unreliable. Nevertheless, $\Delta\Omega$ values of $\Delta\Omega = 0.1868$ and $\Delta\Omega = 0.0608$, translating to equator-lap-pole times of 34 and 103 d, are determined for HK

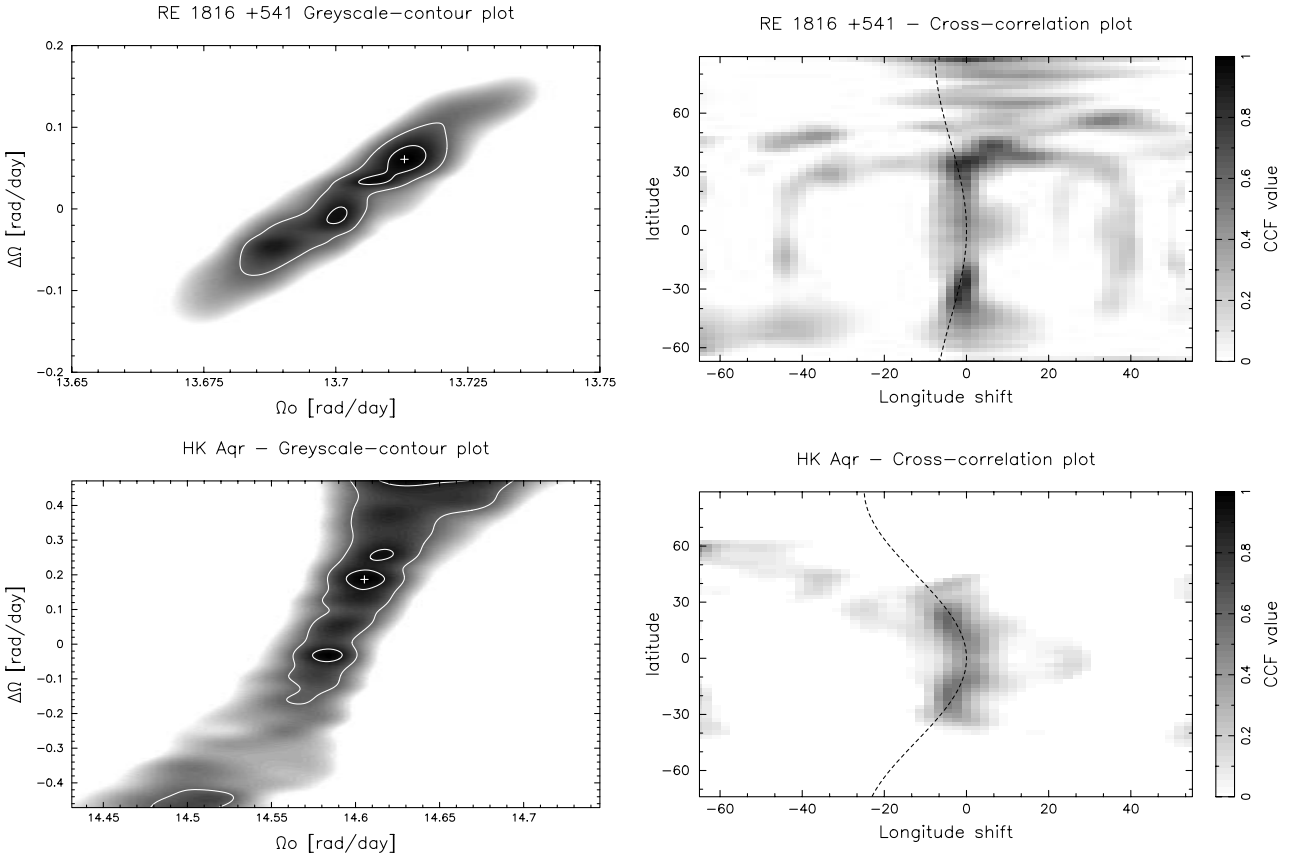

Figure 8. Left: greyscale contour maps of $\Delta\chi^2$ as a function of $\Delta\Omega$ versus Ω_0 for RE 1816 +541 (top) and HK Aqr (bottom). The inner contours mark the 63.8 per cent confidence interval boundaries while the outer contours mark the 99 per cent confidence interval boundaries. The amplitude of the differential rotation values are $\Delta\Omega = 0.0608$ and 0.1868 for RE 1816 +541 and HK Aqr respectively. This translates into respective equator-lap-pole times of 103 and 34 d. Right: cross-correlation images with the fitted differential rotation pattern superimposed.

Aqr and RE 1816 +541. Given the poor S/N ratio of the HK Aqr data this result is probably inconclusive. The RE 1816 +541 measurement is somewhat smaller than the measurable limit of 58 d for the equator-lap-pole time estimated from synthetic data trials as described above. We are therefore unable to give a reliable measure of the differential rotation rate on either star. The possibility of strong differential rotation (equator-lap-pole time ~ 5 d) hinted at in the grey-scale contour map of HK Aqr is physically unlikely, and a probable consequence of the low S/N ratio of the data.

6 CONCLUSION

There has been much interest in recent years over the form of the differential rotation in main-sequence stars. Following the discovery of the region of strong radial shear at the base of the convection zone, models have been produced that can successfully reproduce the latitudinal emergence of magnetic flux on the Sun. Application of the model to rapid rotators suggested that the Coriolis force becomes a dominant factor in the latitude emergence of magnetic flux, and hence it has been predicted that we should see only starspots at intermediate latitudes, and not low latitudes, as on the Sun. Doppler imaging work by a number of authors has, however, shown that starspots usually occur at a range of latitudes, often in distinct latitude bands. Starspots are *not*, however, excluded from low latitudes. RE 1816 +541 also shows starspots at all latitudes, but it is unclear whether they are restricted to well-defined latitude bands. Despite the probable loss of some high-latitude structure owing to poor S/N ratio data, HK Aqr clearly opposes the picture of a solar-type dynamo in a rapid rotator as the majority of reconstructed features appear at low to intermediate latitudes.

It is perhaps noteworthy that of the four latest type dwarfs for which Doppler images exist, Speedy Mic (Barnes et al. 2001), BD +2204 (Lister, Collier Cameron & Bartus 1999), HK Aqr, RE 1816 +541, none other than BD +2204 reveal strong polar caps. In a previous paper it was suggested the waxing and waning of a polar cap and appearance of starspot bands at different latitudes may be a feature of a stellar cycle. Without a statistically reliable sample of objects it remains unclear as to whether there is also a strong dependence on spectral type as the convection zone depth increases. A distributed dynamo seems all the more plausible in the mostly convective M dwarfs. Attempting to construct models that can allow for the build up of flux within the convection zone, over a stellar cycle, may prove difficult, but may be necessary in order to explain the latitudinal distribution of starspots.

It is clear that a number of improvements could be made in the study of largely or fully convective M dwarfs. Better model atmospheres with molecular opacities should assist recovery of a higher S/N ratio profiles. The advent of 8-m class telescopes and more efficient spectrographs on 4-m class telescopes will hopefully greatly widen possibilities. Indeed, this analysis shows that the larger CCD chips now available are also crucial in order to obtain the S/N ratio necessary to reliably constrain images and physical parameters such as differential rotation, if indeed it is significant at such late spectral types. M dwarfs show a lower amplitude of modulation in *V*-band lightcurves, often making period determinations difficult, though not impossible. For this reason the periods of faint M dwarfs in young open clusters remain largely unknown as surveys have concentrated on the brighter members. Wide field surveys of clusters would be an ideal means of determining such periods.

ACKNOWLEDGMENTS

This work is based upon data taken from the AAT and ING data archives. The WHT is operated on the island of La Palma by the Royal Greenwich Observatory in the Spanish Observatorio del Roque de los Muchachos of the Instituto de Astrofisica de Canarias. The AAT is operated by the Anglo Australian Observatory at Siding Spring Observatory.

REFERENCES

Barnes J., Collier Cameron A., Unruh Y., Donati J.-F., Hussain G., 1998, MNRAS, 299, 904
Barnes J., Collier Cameron A., James D., Donati J.-F., 2000, MNRAS, 314, 162
Barnes J., Collier Cameron A., James D., 2001, MNRAS, in press
Bopp B. W., Dempsey R. C., Africano J. L., Goodrich B. D., 1988, PASP, 100, 579
Byrne P. B., Eibe M. T., Rolleston W. R. J., 1996, A&A, 311, 651
Collier Cameron A., Robinson R. D., 1989a, MNRAS, 236, 57
Collier Cameron A., Robinson R. D., 1989b, MNRAS, 238, 657
D'Antona F., Mazzitelli I., 1994, ApJS, 90, 467
Donati J.-F., Collier Cameron A., 1997, MNRAS, 291, 1
Donati J.-F., Semel M., Carter B., Rees D. E., Collier Cameron A., 1997, MNRAS, 291, 658
Donati J.-F., Mengel M., Carter B., Marsden S., Collier Cameron A., Wichmann R., 2000, MNRAS, 316, 699
Eibe M. T., 1998, A&A, 337, 757
Gray D. F., 1992, The Observation and Analysis of Stellar Photospheres. Cambridge Univ. Press, Cambridge
Herbst W., Layden A. C., 1987, AJ, 94, 150
Horne K. D., 1986, PASP, 98, 609
Jeffries R. D., James D. J., Bromage G. E., 1994, MNRAS, 271, 476
Kupka F., Piskunov N. E., Ryabchikova T. A., Stemples H. C., Weiss W. W., 1999, A&AS, 138, 119
Lister T. A., Collier Cameron A., Bartus J., 1999, MNRAS, 307, 685
Mills D., 1994, Starlink User Note 152, Rutherford Appleton Laboratory
O'Neal D., Neff J., Saar S., 1998, ApJ, 507, 919
Pettersen B. R., Lambert D. L., Tomkin J., Sandmann W. H., Lin H., 1987, A&A, 183, 66
Pounds K. A. et al., 1993, MNRAS, 260, 77
Rao A. R., Singh K. P., 1990, ApJ, 352, 303
Robb R. M., Cardinal R. D., 1995, Informational Bulletin on Variable Stars, 4270, 1
Soderblom D. R., Stauffer J. R., Hudon J. D., Jones B. F., 1993, ApJS, 85, 315
Vogt S. S., Penrod G. D., 1983, PASP, 95, 565
Young A., Skumanich A., Harlan E., 1984, ApJ, 282, 683
Young A., Skumanich A., MacGregor K. B., Temple S., 1990, ApJ, 349, 608

This paper has been typeset from a TEX/LATEX file prepared by the author.